

# Filtration-induced pressure evolution in permeation grouting

Zilong Zhou<sup>1a</sup>, Haizhi Zang<sup>1,2b</sup>, Shanyong Wang<sup>2c</sup>, Xin Cai<sup>\*1d</sup> and Xueming Du<sup>3e</sup>

<sup>1</sup>School of Resources and Safety Engineering, Central South University, Changsha 410083, People's Republic of China

<sup>2</sup>Faculty of Engineering and Built Environment, ARC Centre of Excellence for Geotechnical Science and Engineering, The University of Newcastle, Callaghan 2308, Australia

<sup>3</sup>College of Water Conservancy and Environmental Engineering, Zhengzhou University, Zhengzhou 450001, People's Republic of China

(Received December 5, 2019, Revised January 16, 2020, Accepted March 15, 2020)

**Abstract.** Permeation grouting is of great significance for consolidating geo-materials without disturbing the original geo-structure. To dip into the filtration-induced pressure increment that dominates the grout penetration in permeation grouting, nonlinear filtration coefficients embedded in a convection-filtration model were proposed, in which the volume of cement particles in grout and the deposited particles of skeleton were considered. An experiment was designed to determine the filtration coefficients and verify the model. The filtration coefficients deduced from experimental data were used in simulation, and the modelling results matched well with the experimental ones. The pressure drop revealed in experiments and captured in modelling demonstrated that the surge of inflow pressure lagged behind the stoppage of flow channels. In addition, both the consideration of the particles loss in liquid grout and the number of filtrated particles on pore walls presented an ideal trend in filtration rate, in which the filtration rate first rose rapidly and then reached to a steady plateau. Finally, this observed pressure drop was extended to the grouting design which alters the water to cement (W/C) ratio so as to alleviate the filtration effect. This study offers a novel insight into the filtration behaviour and has a practical meaning to extend penetration distance.

**Keywords:** filtration rate; pressure evolution; cement grout; penetration distance; water to cement ratio

## 1. Introduction

Permeation grouting is a widely used technique that solidifies the loose geo-structure and reduces the permeability. Compared with the chemical grouting with a potential risk of pollution transported to groundwater (Sui *et al.* 2015; Cai *et al.* 2019) and the low stability under extreme conditions such as high/low temperature (Esfte *et al.* 2016; Bohlooli *et al.* 2018; Wang *et al.* 2019), sedimentation erosion (Nouri and Heydari 2017) or external dynamic disturbance (Li *et al.* 2012; Zhou *et al.* 2018; Zhang *et al.* 2019; Zhou *et al.* 2019; Zhu *et al.* 2019), cement-based grout has been adopted in various civil engineering due to its low cost and environment-friendly properties (Im and Hurlbaas 2012). An indispensable weakness of permeation grouting is its low penetration distance derived from the limited driven source, as over-high flow rate or pressure may bring about the matrix fracturing (Park and Oh 2018) and the leakage of grout into undesigned area (Liu *et al.* 2018; Wang *et al.* 2020). In the grouting process, the spatial pressure evolving with grouting time is a crucial factor that instructs the practical engineering, and a thorough

understanding of this complex process will introduce new insight into permeation grouting design.

The filtrated cement particles, which deposit on the pore surface of skeleton and narrow the flowing channel, should be responsible for the pressure increment. It is usually believed that Bingham fluid ceases flowing when the pressure gradient in front of penetrating fails to satisfy the yield condition (Axelsson *et al.* 2009; Dang *et al.* 2019), and then a plug spreading out the cross-section area of flowing passage blocks the pores by occupying grouting liquid (Zou *et al.* 2018). This criterion is applicable to low water to cement (W/C) ratio of grout that is usually used to seal the large aperture of rock fracture (Zou *et al.* 2019; Zou *et al.* 2020) or high-porosity gravel material with large grain size; while for regular soil and sand porous media, the gradual loss of cement particles (Fan *et al.* 2018) and deposited particles onto skeleton dominate the porosity decline and the pressure evolution.

Because of the unobservable penetration process inside the porous media, a phenomenological deduction based on the continuous evolution of pressure is usually utilized to dip into the filtration coefficient (Bouchelaghem 2009; Yan *et al.* 2017). Driven by hydraulic force, cement particles flow synchronously with the liquid phase and are generally regarded as the same velocity with the liquid in continuum model (Song *et al.* 2018; Song *et al.* 2018). The velocity of grout front can be successively monitored by using the camera CCD (Bouchelaghem and Almosni 2003; Zhou *et al.* 2019) to infer other parameters in flowing equation, while the filtration process in the cement-filled area cannot be observed. An alternative is to regard the whole geomaterial-filled experimental container as a single collector, in which

\*Corresponding author, Associate Professor

E-mail: [xincai@csu.edu.cn](mailto:xincai@csu.edu.cn)

<sup>a</sup> Ph.D., Professor,

<sup>b</sup> Master Student

<sup>c</sup> Ph.D., Professor

<sup>d</sup> Ph.D., Associate Professor

<sup>e</sup> Ph.D., Post-Doctoral Fellow

the filtration coefficient is seen as a constant (Yoon and El Mohtar 2015) or a variable varying with time (Zhou *et al.* 2018). This assumption may be applicable in a relatively small unit where filtration effect is less intense to completely block the flowing passage, while for a long one-dimensional container or two-dimensional radial flow condition which has much longer available penetration distance than its width or diameter, extremely non-uniform filtration behaviour appears and the linear assumption regarding the relation between the concentration of cement grout and filtration rate breaks up (Zhou *et al.* 2018). Generally, the determination of filtration coefficient lies at a wide range of factors (Tien and Payatakes 1979), among which the volume of cement particles and the specific deposition of cement particles play a vital role. The interstitial velocity is another important factor while its influence is embedded in the variation of porosity as it varies inversely with the porosity under the constant injected flow rate. To simplify the representation of filtration coefficient, cement particles are deemed to be captured by the pore wall once they contact with each other. However, some discrete simulation in pore network model reveals that the scouring and mounding of deposited particles possess a huge impact on filtration rate (Kim and Whittle 2009; Yang and Balhoff 2017).

The surge of inflow pressure is a widely acceptable principle of ceasing grouting process, but the unstable development and variation of pressure give rise to more uncertainties that damage the structure of porous media. An early stop of grouting may fails to reach the designed target of improving constructions, while a late termination would probably fracture the matrix and create new flow channel that leaks the injected grout (Kou *et al.* 2019). Although some successful predictions of pressure evolution have been made (Moghadasi *et al.* 2004; Kim *et al.* 2009; Zhou *et al.* 2018), the pressure drop after the stoppage has been barely mentioned (Ghafar *et al.* 2018; Zhou *et al.* 2019). As a matter of fact, the inflow pressure drop happens in company with the massive blockage of pore channels in near-inlet area, which lags behind the intersection of grout flow after the blockage area. This phenomenon has the potential for revealing the stoppage mechanism and predicting the stoppage point that helps judge the effective penetration distance.

To probe into the spatial pressure evolution caused by filtration behaviour in permeation grouting, a filtration model considering the loss of cement particles and specific deposition was proposed and an elaborate experiment along with a simulation were designed to verify the model. In addition, the variation of filtration rate related to the volume of cement particles and the deposited particles of skeleton was discussed. Finally, the corresponding pressure drop along the penetration distance was revealed and then be bridged with some approaches to alleviate the filtration effect in permeation grouting.

## 2. Model description

### 2.1 Convection-filtration model

The transport of grout in porous media can be divided

into two components: water flow and particle transport (Zhou *et al.* 2019). Pressure-driven source provides hydrodynamic force for liquid flowing, while cement particles (Yang and Balhoff 2017) are carried on by fluid. The movement of particles are mainly influenced by convection, diffusion, mechanical dispersion, sedimentation, and other microscale forces (Vaz *et al.* 2017). Among these factors, convection plays a dominant role in driving the movement of particles (Sanderson *et al.* 2018). Molecule Diffusion and mechanical dispersion constitute the hydrodynamic dispersion, which can be neglected if the size of particle is between 10 and 50  $\mu\text{m}$  or higher (Yoon and El Mohtar 2014). Sedimentation of cement particles is attributed to the aggregation of individual particles, it can be mitigated if certain chemical admixture is added to reduce the number of bulk particles; as for the electrical forces, Von Der Waals force or Brown motion, they are difficult to be observed in laboratory tests and their corresponding disturbance on the filtration coefficient only have limited impact (Kim and Whittle 2009). Another factor in permeation grouting is the skeleton deformation (Ebrahimi and Barati 2018). Generally, to avoid the further damage on injected porous media in practice, grouting flow rate or pressure are adjusted to under certain value, as well as reducing the swelling of skeleton. Also, measuring data reported by Bouchelaghem *et al.* (2001) shows that the strains of porous matrix are roughly at the order of 10<sup>-6</sup>. Therefore, only convection and filtration effect are considered in this paper, and the velocity of water, cement particles and grout are assumed to be the same.

The classical equation Darcy's law, describing fluid flow in porous media as:

$$u = -\frac{k}{\mu}\nabla p \quad (1)$$

where  $u$  is the superficial velocity of filtered porous media,  $k$  is the permeability of filtered porous media,  $\mu$  is the viscosity of grout, and  $\nabla p$  is the pressure gradient. It should be noticed that the grout is regarded as a Newtonian liquid at a macroscopic scale. Many laboratory tests show that the grout flows in a Newtonian behaviour when the W/C ratio is over 1.5 or 2 (Wang *et al.* 2018; Zhou *et al.* 2018). Non-Newtonian assumption is also applicable to the Darcy's law as long as the analytical expression of shear force with shear rate is available. Additionally, Darcy's law is valid when the Reynold number is under 5 or a lower limit, otherwise Stokes-Brinkman equation or other high-speed flow equations should be adopted (Ma *et al.* 2016; Zhou *et al.* 2018).

With the accumulation of cement particles inside the porous voids, the porosity of porous media decreases gradually, and the filtration rate (the change in porosity with time) can be expressed as:

$$\frac{\partial \phi}{\partial t} = -\frac{\partial \sigma}{\partial t} = -\frac{\phi_0 - \phi}{\partial t} \quad (2)$$

where  $\phi$  and  $\phi_0$  are the porosity and initial porosity of porous bed,  $\sigma$  is the specific deposition of skeleton, in other words, the volume of deposited cement particles per volume of bed.

The filtrated particles come from the loss of cement

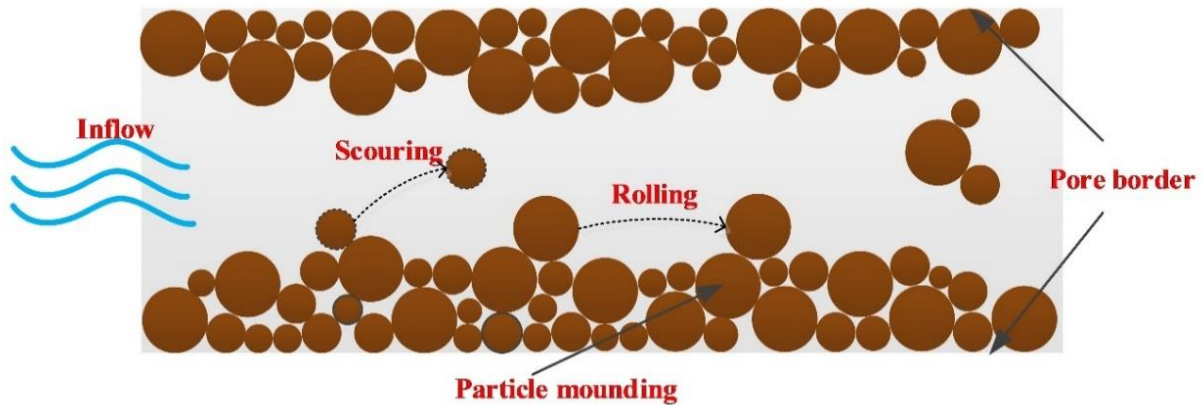


Fig. 1 Schematic drawing of scouring and rolling of cement particles during filtration

particles in grout. Assuming a saturated grout flow in porous media, which means all voids are occupied with liquid, then the mass balance in grout should satisfies (Saada *et al.* 2005):

$$\frac{\partial(\phi\delta)}{\partial t} + \mathbf{u} \cdot \nabla\delta = -\frac{\partial\sigma}{\partial t} \quad (3)$$

where  $\delta$  is the volume ratio of cement particles to bed voids.

The viscosity of grout usually varies linearly with the concentration of cement particles (Kim and Whittle 2009), we simplify it to a linear relationship with the volume rate  $\delta$ :

$$\mu = \mu_w \left( 1 + \left( \frac{\mu_0}{\mu_w} - 1 \right) \frac{\delta\phi}{\delta_0\phi_0} \right) \quad (4)$$

where  $\mu_w$  is the viscosity of water,  $\mu_0$  and  $\delta_0$  are the initial viscosity and volume rate of cement particles before injection.

The permeability of bed decreases with the reduction of porosity. Generally, the diverse void throats (Yang and Balhoff 2017) that connect flowing channels, the relative angle between fluid flow and gravity, and the deposition morphology (Kim and Whittle 2006) are decisive in the variation in permeability during grouting process. With few laboratory evidence to quantify these factors, the classical Kozeny-Carman equation, which considers the grain size of porous media, is widely used in pressure drop prediction regarding the flowing through a packed bed. The factor of grain size in original equation is embedded in the initial permeability and we adopt a smooth deposition of particles is adopted in this paper (Bouchelaghem *et al.* 2001):

$$k = k_0 \left( \frac{\phi}{\phi_0} \right)^3 \left( \frac{1 - \phi_0}{1 - \phi} \right)^{3/4} \quad (5)$$

where  $k_0$  is the initial permeability of porous bed before injection.

## 2.2 Filtration coefficients

The loss of cement particles and the reduction of porosity lead to the narrowness of flowing channels in

porous media. This process in turn disturbs the grout flowing and particles adsorbing. Several investigations dip into the microscale movement of cement particles by discrete simulation (Kou *et al.* 2019; Liu *et al.* 2019), considering the pore shape, pore angle, throat connection and etc. Despite the fact that these elaborated descriptions provide an insight into the filtration behaviour theoretically, abundant parameters in simulation can hardly be linked to the macroscopic observation or measurements that are more approachable (Wang *et al.* 2018; Kou *et al.* 2019; Song *et al.* 2019; Wang *et al.* 2019). In this section, we focus on the determination of filtration coefficients which play an important role in porosity reduction, in a macroscopic description involved with measurable data of bed porosity and grout viscosity.

The deposition of cement particles on skeleton, scouring and rolling of adsorbed particles are taken into account to decide the filtration coefficient. Generally, the filtration rate is positively correlated with the volume of cement particles; while high interstitial velocity has adverse effect on filtration, since individual particle undertakes larger hydraulic driven force compared with low flowing velocity. As the ongoing deposition and further mounding of cement particles, as shown in Fig. 1, particles on the surface of the mounding might be scoured or rolled towards the flow direction. Scoured particles come back to flowing grout and thus widen the vacant pore space; while rolling ones from original positions further occupy pore space where the rolling particles reach. Which of these two processes dominates would decide whether more or less pore space appears. We leave this dynamic balance in future work and concentrate on the overall variation in filtration coefficients.

According to the aforementioned relationship among volume of cement particles and the particle migration, the filtration rate can be expressed as:

$$\frac{\partial\sigma}{\partial t} \propto \phi_c, \phi_0 - \phi \quad (6)$$

where  $\phi_c$  is the volume of cement particles per volume of porous bed.

Using the first order for the Taylor expansion, we can obtain:

$$\frac{\partial \sigma}{\partial t} = \lambda_l \phi_c + \lambda_d (\phi_0 - \phi) \quad (7)$$

where  $\lambda_l$  and  $\lambda_d$  is the loss rate of cement particles from grout and the dynamic variation rate of deposited cement particles respectively. With the narrowness of pore space, the probability of particles deposition rises gradually (Reddi and Bonala 1997); similarly, the more particles accumulated, the less intense the scouring and rolling effects are, since the individual particle is less likely to be dragged away if it is cemented in aggregation (Yang and Balhoff 2017). Hence, Eq.(7) is rewritten as:

$$\frac{\partial \sigma}{\partial t} = a\phi_c + \frac{c\Delta\sigma}{1 + b\Delta\sigma} = a\delta\phi + \frac{c(\phi_0 - \phi)}{1 + b(\phi_0 - \phi)} \quad (8)$$

where a, b, c are fitting constants.

Compared with the traditional filtration coefficient, the proposed filtration coefficients considers both the particle deposition on skeleton and the loss the deposited particles during grout scouring in pore space, which is competent to represent the dynamic variation of nonlinear filtration rate instead of the linear filtration rate in previous work. Actually nonlinear evolution of filtration rate turns into more intense when it comes to the high-speed grout flow or approaching the nearly stoppage stage, it is necessary to cover these factors.

The combination of the governing Darcy's flow Eq. (1), mass balance equations of Eq. (2) and Eq. (3) can be simplified into two partial differential equations and a flow equation which can be solved in Comsol. Only one-dimensional geometry is considered for simplification, while it is easily extended to multi-dimension problems presented by a representative elementary volume (REV) scale (Bouchelaghem 2009).

According to the known porosity varying with time at different locations along the penetration distance, the filtration rate can be roughly estimated by the average of forward differences and backward differences at different sampling time points:

$$\Delta\dot{\sigma}_{i,j} = \frac{1}{2} \left( \frac{\phi_{i,j} - \phi_{i-1,j}}{\Delta t_{i-1,i}} + \frac{\phi_{i+1,j} - \phi_{i,j}}{\Delta t_{i,i+1}} \right) \quad (9)$$

where  $\phi_{i,j}$ ,  $\phi_{i-1,j}$ ,  $\phi_{i+1,j}$  represent the porosity of the location of  $j$ , at the sampling time point  $i$ , preceding the sampling time point and after the sampling time point respectively.  $\Delta t_{i-1,i}$  (or  $\Delta t_{i,i+1}$ ) is the time interval between the sampling time point and its previous (or following) sampling time point. The above approach for calculation considers the rapid variation in porosity in particles filtration, and it reduces the error under the condition of lacking the abundant porosity data in time order.

The aforementioned simplification is also applicable to the estimation of the volume of deposited cement particles at different sampling points:

$$\Delta\sigma_{i,j} = \frac{2\phi_0 - (\phi_{i,j} + \phi_{i-1,j})}{2} \quad (10)$$

It should be noticed that the volumetric increment of deposited cement particles takes the porosity at previous

sampling time point into account instead of only using the porosity at the sampling time point, which diminishes the error that comes from the large time interval of sampling and the rapid variation in filtration rate. However, further simplification on the volume of cement particles is not adopted, because the collection of grout covered a relative wide area near the sampling point and it can represent the regional viscosity. Unnecessary backward difference or forward difference may counteract the change in viscosity that is quantified by the sparsely measuring data. Consequently, the constants a,b,c in Eq. (8) can be decided based on the least square method by minimizing the following equation:

$$f(a, b, c) = \sum_i \sum_j \left( a\delta_{i,j}\phi_{i,j} + \frac{b\Delta\sigma_{i,j}}{1 + c\Delta\sigma_{i,j}} - \Delta\dot{\sigma}_{i,j} \right)^2 \quad (11)$$

### 3. Experimental Investigation and verification

#### 3.1 Set-up and materials

In traditional grouting experiments, porous media container is usually regarded as a single collector which functions as a completely sealing container instead of the combination of separated segments (Markou *et al.* 2015). Although pressure sensors are placed at different locations to investigate the pressure evolution, it is still difficult to dip into the spatial variation of porosity and viscosity experimentally. In this study, in order to obtain the porosity and viscosity along the penetration distance, we adopted a segmented container which consists of six steel-wall cylinders. As shown in Fig. 2, each segment with 30 cm in length and 8 cm in inner diameter is bolted together along the axial direction to constitute a 180 cm cylindrical container. Each segment has a valve hole to collect grout, as well as a pressure sensor to measure the grouting pressure. Portland cement (PO.42.5) with a fineness of 330-410m/kg<sup>2</sup> was used. Negative pressure sieving method was adopted to obtain the cement material with a maximum particle size of 80  $\mu\text{m}$  and average size of 65  $\mu\text{m}$ . To improve the flowability and ensure the stability of the cement grout, water and chemical admixtures were poured in a churn barrel (300 mm in diameter and 450 mm of height). The cement was introduced into the barrel with water over a period of 1 min at a rotation velocity of 400 r/min. Then, the mixture has been mixed for 10 min in three stages: 4 min at 400 r/min, 2 min at 300 r/min and 4 min at 400 r/min. The properties of used sand can be seen in Table 1.

#### 3.2 Experimental Procedure

Several groups of tests with different grouting parameters were conducted before the experiment, to choose the most proper combination that can penetrate the longest distance (Zhou *et al.* 2019). The aim is to make sure that all measuring parameters are accessible at each location and time point. Accordingly, the water/cement (W/C) ratio was set as 1.5 with a stable grout viscosity of 17.1  $\text{mPa} \cdot \text{s}$ , and the constant flow rate of the grout injection was 2.35

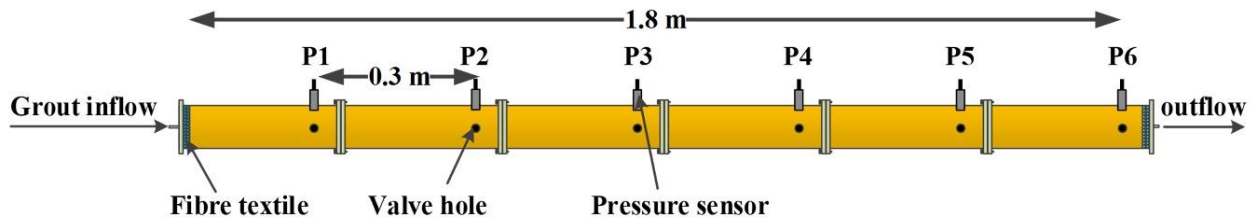


Fig. 2 Schematic diagram of experimental set-up

$L/min$  realized by a constant-power pump. To avoid the variation in grout rheology with time, the longest duration of the experiment was controlled no more than 60 s. Another reason we chose 60 s as the final experimental time is that some porous channels were completely blocked up and the grout actually ceased flowing after this time point in most groups of experiments. To remove the air in sand, water was injected before each test.

Data of grout viscosity and porosity were collected at the six measuring points (P1 - P6). Valve holes were opened at different locations to collect filtrated grout at designed time points (10s, 30s and 60s), then the rotary viscosity metre was used to gain the viscosity data along the penetration distance. The scope of rotary viscosity metre was set as 0–100 mPa s, which was realized by a rotor of  $\phi 1.88 \times 7.07$  mm and a rotate speed of 60 r/min. The viscosity data was read until it did not change any more within 10 seconds. After each group of test, the whole container was dismantled into six separated ones and a PVC pipe with an inner diameter of 63 mm was squeezed into the cemented sand to obtain a cylinder sample. After 28 days, the samples from six segments were processed into small samples with 30 mm in diameter and were immersed in water for 24 hours. Then we used nuclear magnetic resonance (NMR) technique to measure the porosity. Due to the damage on injected porous media from porosity measuring method and the loss of liquid grout at each measuring time in experiments, we abandoned the injected sand and refilled clean sand after manually collecting data of viscosity in each test. It should be noticed that the accuracy of data not only depends on the technique adopted, but also the sampling time interval. To alleviate the unnecessary manual error regarding the measuring time and terminating time, as it mentioned before, only three groups of time were considered, that is to say, 10 s, 30 s and 60 s. While the pressure data were collected automatically by computer, which changed from 10 s to 60 s by 10 s increment.

### 3.3 Filtration-induced Particle Loss and Pressure Increment

The variation in grout viscosity is related to the change in the volume of particles in the flowing grout (Shabani *et al.* 2019). As shown in Fig. 3, from the near-injected location P1 to P6 by the outlet, only a slight change in viscosity is seen during the first 10 s, which means the flowing grout only loses few particles; while the filtration

Table 1 Grain size distribution of sand

Grain size proportion (%)						Bulk density ( $kg/m^3$ )	Grain density ( $kg/m^3$ )
.05 mm	.15 mm	.2 mm	.4 mm	.6 mm	1.2 mm		
2.8	7.8	14.3	16.4	23.6	35.1	1740	3028

effect escalates into a rapid fall of viscosity at 30 s, and the far-inlet locations present severer particle loss. This process continues evolving until a specific area in front of P3, at which all flow passages inside the porous media are blocked, forms a cemented cake that consists of the accumulating particles aggregation. It also means that the effective penetration does not continue beyond the location of P3.

Further evidences of particle loss can be seen in Fig. 4, which shows that the lost particles deposit on the skeleton of porous media and gradually decrease the porosity. The variation in porosity roughly presents the reversed trend of that in viscosity. The near-inlet locations before P3 experience unevenly porosity drops, and the closer to the inlet, the larger in the decline. The steady change in porosity during the first 10 s accords to the variation in viscosity at the same period. Subsequently, the porosity at P1 and P2 decline dramatically, in which the figure at P1 of 60 s drops to only 0.12. By contrast, the flowing stop point of P3 (inferred from Fig. 3) still has a high porosity over 0.32, which demonstrates that only a small area before P3 is cemented effectively but a large area after this position fails to be reinforced. It should be noticed that the porosity of 0.12 could either be the stoppage porosity or locate farther than the stoppage point. The cement particles might block channels preceding this measuring point or only partial sections reach completely blockage, which leaves more porous voids after this point. It is not reasonable to regard the value of 0.12 as the stoppage porosity without dense porosity data close to the stoppage point.

Grouting pressure is a vital factor that decides whether or not to terminate the grouting process in practical engineering. The pressure rises with the reduction of effective cross-sectional area, because more driven pressure are necessary to keep the constant flow rate when the flow channels are narrowed. The rapid growth and the sudden drop of pressure can be seen in Fig. 5. The near-inlet locations have higher pressure due to the lower porosity. Different from the linear increase observed in previous studies (Bouchelaghem *et al.* 2001; Maghous *et al.* 2007; Xu and Bezuijen 2019), the pressure after the location of P1 first grow gradually and then fall down. The stoppage point

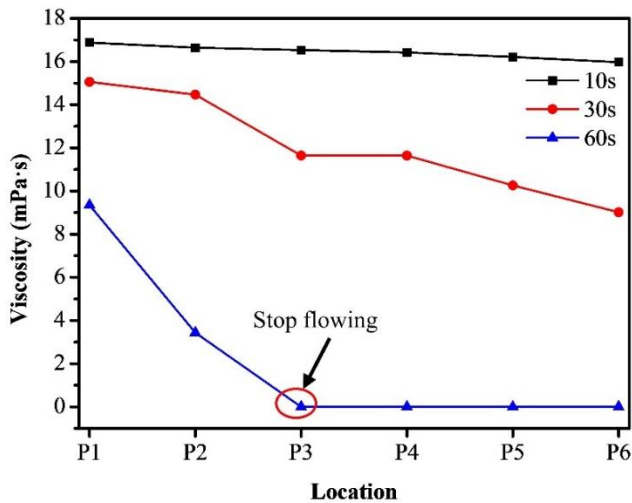


Fig. 3 Variation in grout viscosity due to particle loss

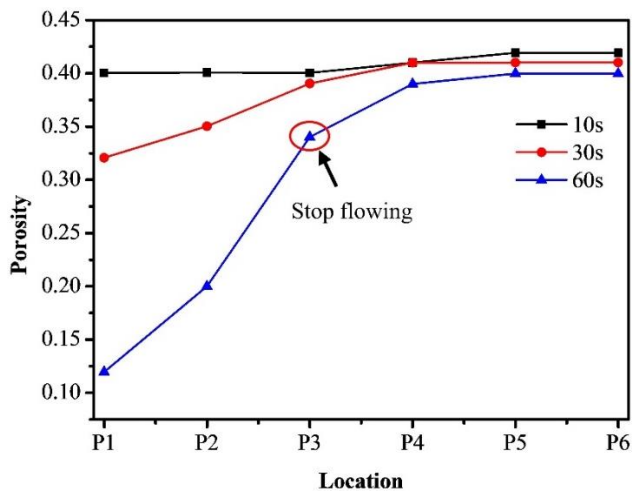


Fig. 4 Variation in porosity due to particle filtration

can be inferred from the drop point closest to the inlet, which is at P2 and occurs at 50 s. The reason for this phenomenon is that the cemented cake obstructs the flow channels and cuts off the source that supplies grout for the following locations. This peculiar fact shows that even we can take the inflow pressure as a reference to judge the termination time of grouting, it does not represent that the perfect penetration distance has been achieved.

The pressure drop at the location far from the inlet appears earlier than other near-inlet ones. The successive pressure drops along the grout penetration are shown in Fig. 5. P5 and P6 occur pressure drop at 20 s, followed by P3 and P4 at 30 s. The final drop point lies at the location of P2 when grout penetration proceeds to 50 s. This trend is in line with the variation in porosity which presents the huge difference of porosity between P2 and P3. As mentioned above, based on the closest drop point to inlet, the effective penetration distance can be inferred. This criteria may contradict with that from empirical formulas which assume a uniform diffusion of cement grout in porous voids (Chupin *et al.* 2008). Due to the unclear filtration mechanism of cement particles, the partial consideration of liquid rheology (Yoon and El Mohtar 2014) and convection

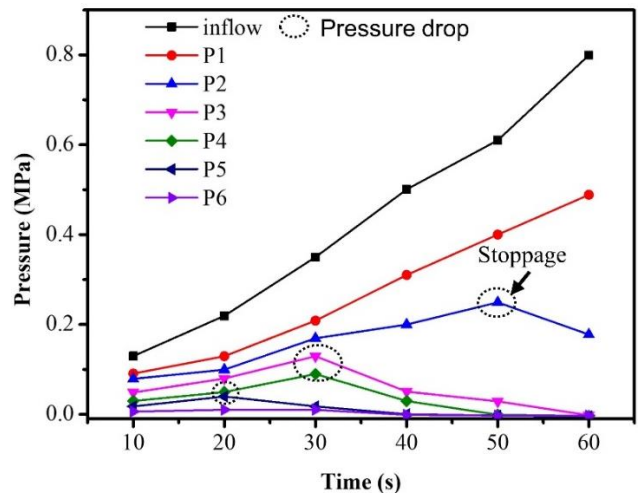


Fig. 5 Spatial and temporal variation in grouting pressure

### 3.4 Verification of Porosity and Pressure

might not obtain the ideal penetration distance. In spite of the far extension of grout front, part of the spreading area or most of them is limitedly filled, which is unable to solidify the whole porous media effectively. Understanding the behaviour of pressure drop provides a new angle into the permeation grouting, without further microscale explanation for the exchange of cement particles between grout liquid and porous skeleton.

The proposed model is verified and compared with the experimental porosity and pressure evolution (shown in Fig. 6). It should be noticed that the inflow rate of grout is adjusted in modelling since the original injection rate in experiments is too low to penetrate the whole collector within 60 s. Despite the observed grout flow at different sampling time points during tests, it results from the unsaturated flow of grout through the preferential migration channel (Hou *et al.* 2018). While this imposes minor impact on the parameter determination as the cross-sectional areas of the available flowing passages along the penetration distance are almost consistent, which means the filtration rate has tiny disturbance regardless of the diameter of collector. As shown in Fig. 6(a), the extent of deviation between modelling and experimental results heightens with time, while overall these two trends correspond with each other. A main reason should be responsible for this deviation is that the smooth deposition (Reddi *et al.* 2005) instead of various deposited morphology (Kim and Whittle 2009) is considered in this model. In fact, the variation of pore length and the various shapes of throats that connect pores pose great influence on the deposition morphology. Some pores are impenetrable once the near-inlet part are blocked (also called interception), although a large part of the pores after the stoppage point are still vacant. The non-uniform deposition may give rise to the status that only a small portion of cement particles are able to block the whole cross section, and thus brings about a larger porosity reduction in experimental observation. Another possible reason is that the relation between the permeability and the porosity (Eq. (5)) adopted in the model disregards the fact

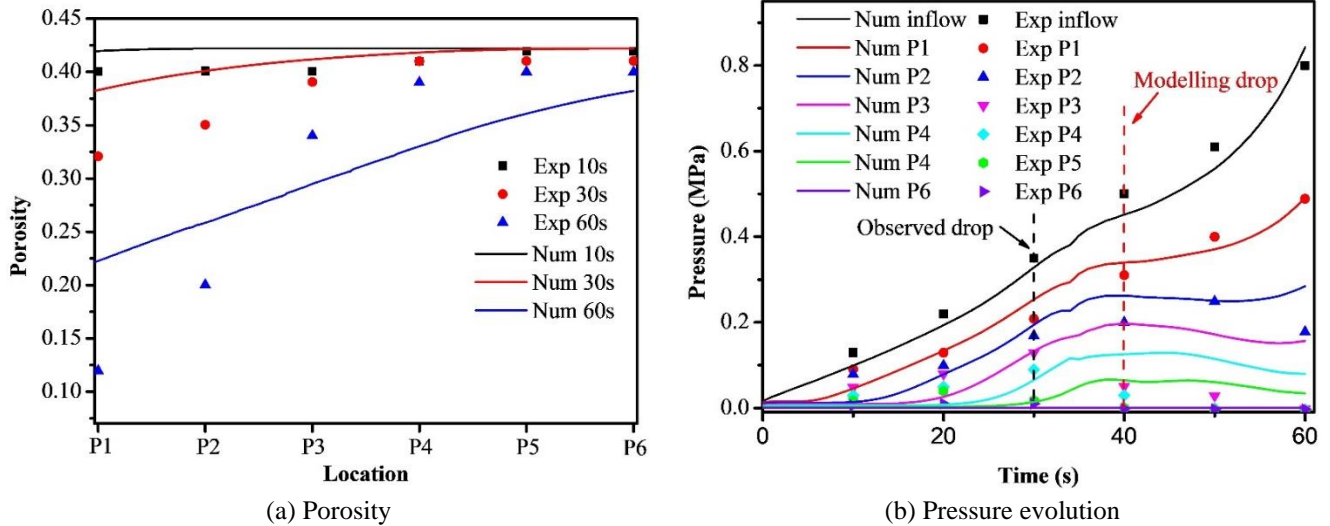


Fig. 6 Comparison of experimental results and modelling results ( $k_0 = 2 \times 10^{-9}$ ,  $\phi_0 = 0.422$ ,  $\delta_0 = 0.4275$ ,  $u_{injection} = 0.02 \text{ m/s}$ )

that a slight disturbance in porosity may introduce a great decrease in permeability when the porosity is quite low (Ma *et al.* 2018). This huge variation depends on the pore structure of porous media and it can be experimentally measured with a group of permeability data varying with porosity under external compression or other methods that measure the porosity evolution (Ma *et al.* 2019). These are why our results seem to be higher than that from experiments. These problems may be addressed if large computational efficiency is available for modelling cement particles transport in pore scale, while they are not the main concern of this study.

The modelling pressure evolution in Fig. 6(b) agrees well with the experimental ones at the locations of P1, P2. The pressure at other sampling points fluctuates after 30 s. The modelling results fails to capture the sudden pressure drop in experiments at 30 s while presents a gradual decrease at 40 s in the following period for P3, P4, P5 and P6. As discussed in section 3.3, the fall of pressure is attributed to the rapid stoppage in near-inlet area that reduces the further supply of cement grout to partly cement-filled area. Due to the existence of the lowest porosity that porous media can reach, the grout might cease flowing completely even the porosity stays a relatively high value, which contributes to an earlier pressure drop in experimental results.

However, the pressure drop lagged in modelling results still shows the overall trend of pressure evolution. A pressure plateau is seen at 40 s after the location of P3 in modelling results, which can be regarded as a criterion to evaluate the penetration distance of cement grout. With the continuous pressure growth near inflow (at P1 and P2) resulting from the rapid reduction in porosity, the effective penetration distance can be preliminarily estimated. The successive pressure plateaus after P2 further demonstrate that the reinforcing area is not beyond P2. An extra evidence is that the porosity (shown in Fig. 6(a)) at P3 is observed to be lowered to only 0.33 at the end of tests, while the porosity at P2 is 0.2 after the injection. Although

the gradual decline happens later at 50 s in modelling, we can judge the modelling drop based on a series of steady fluctuation at around 40 s (Fig. 6(b)).

Given that the filtration coefficients are derived from the sparse experimental data, the less intense filtration-induced pressure growth before the stoppage can be captured closely; while the abrupt pressure drop that happens in a short time once after blockage is difficult to match unless sufficient data of viscosity and porosity at this stage are available. In practice, elaborate laboratory tests are necessary preceding the application of grouting if precise prediction of pressure evolution is required (Song *et al.* 2018; Wang *et al.* 2019; Zhang *et al.* 2019; Song *et al.* 2020).

## 4. Further Investigation with the Proposed Model and Discussion

### 4.1 Linear filtration rate

The embedded filtration coefficients in convection-filtration model includes the linear component ( $a$  in Eq. (8)) and nonlinear components ( $b, c$  in Eq. (8)). The assumption of linear filtration rate is usually adopted in permeation grouting modelling, in which the filtration coefficient related to the volume of cement particles ( $a$  in Eq. (8)) is a constant. However, this criterion would probably introduce error during the late-term grouting process. A preliminary assessment based on the assumption of linear filtration rate adopted in (Saada *et al.* 2005) is shown in Fig. 7. It is noticed that the deviations widen gradually with time, and the same modelling trend appearing in (Saada *et al.* 2005) validates the availability our calculation as well. Without the data of spatial variations in porosity and viscosity in original experiments, the nonlinear exponents ( $b$ , and  $c$  in Eq. (8)) are unapproachable. Actually, the constant filtration rate is only available during the initial filtrated period in which the change in porosity is less intense. With the massive

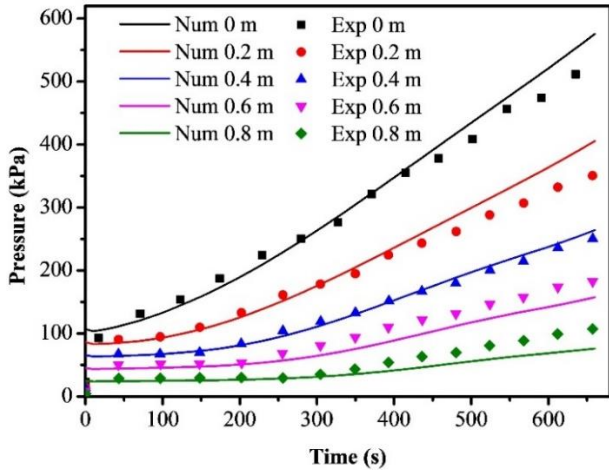


Fig. 7 Comparison of pressure evolution in experiments (Saada *et al.* 2005) and modelling results based on the assumption of linear filtration rate ( $a = 3.06 \times 10^{-3}$ ,  $b = 0$ ,  $c = 0$ )

accumulation of cement particles, the volume loss of cement particles per second may reach a stable level rather than increasing with no upper limit. While the maximum porosity in original experiments falls down to only 0.315 at the end of tests, a roughly 12.5% decrease compared with the initial porosity. Although the linear assumption is able to simplify the representation of filtration behaviour, the rapidly growing filtration rate during the late-term injection may result in a major error.

Another possible factor for the error is attributed to the utilization of single collector which has been widely adopted in various filtration experiments. It is acceptable for some containers if the ratio of length in containers and the characteristic length of porous media is greater than a certain value (Markou *et al.* 2018), afterwards the variation in porosity along the penetration distance may vary greatly because of the non-uniform filtration effect in different locations. As discussed in (Zhou *et al.* 2018), the filtration rate fluctuates drastically as further stoppage of flowing channels occurs, and the deposited cement particles (or the reduction of porosity) gradually dominate the filtration. Therefore, taking the variation in filtration coefficients along the penetration distance into account instead of looking at the whole container as a unit is necessary.

#### 4.2 Nonlinear filtration rate

According to the known porosity and grout viscosity varying with distance and time in experimental tests of this study, the evolution of filtration rate with the volume of cement particles  $\delta\phi (= \phi_c)$  and the porosity reduction  $\phi_0 - \phi$  is presented in Fig. 8. It is clear that the filtration rate varies greatly with these two variables, rather than being a linear relation with the volume of cement particles. The relationship between the filtration rate and  $\delta\phi$  does not present a strong relevance. The overall trend is that the higher volume rate of cement particles shows relatively weak filtration effect, while this trend blurs when  $\delta\phi$  ranges from 0.08 to 0.14. It might contradict the speculation

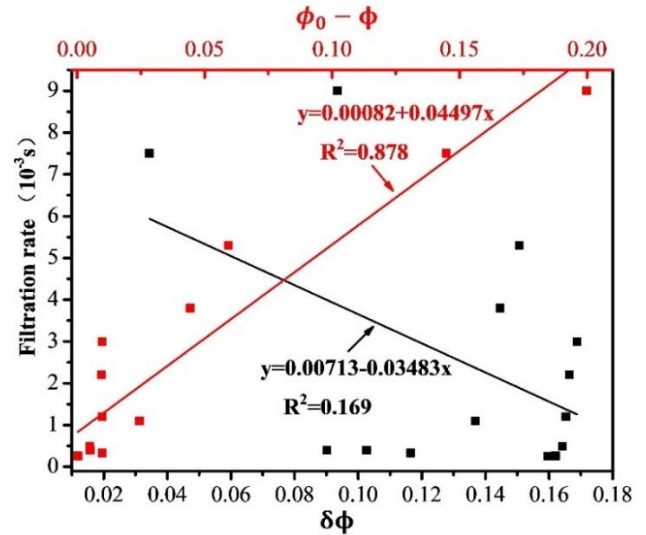


Fig. 8 Filtration rate varies with the volume of cement particles and specific deposition of skeleton

that high volume rate of cement particles, that is to say, more cement particles per volume of pore channel, would facility the deposition of particles and intensify particles movement. This derives from the partial consideration of the number of cement particles, while neglecting the impact from deposited particles. The red line in Fig. 8 further demonstrates that accumulated cement particles contribute to the particles deposition. However, the growth in filtration would not continue since fewer cement particles could enter the flowing channel narrowed by deposited particles.

Based on the determination of constants in Eq. (8), the adopted nonlinear evolution of filtration rate in calculation is shown in Fig. 9. The increase in filtration varying with volume of cement particles under the same specific deposition of skeleton tends to be slow, which roughly accords to the constant filtration coefficient observed in some experiments or simulations (Saada *et al.* 2005; Chupin *et al.* 2008; Yoon and El Mohtar 2015). When it comes to the growth of filtration rate under the same volume of cement particles, a much stronger surge appears compared with the change that relates to the volume of cement particles. This trend well explains that the filtrated cement particles dominate the filtration behaviour especially under large accumulation condition as few cement particles can flow through the porous channel. In addition, it indicates that it is not reasonable to decide filtration rate by singly involving either the volume of cement particles or the specific deposition of skeleton, combination of these two factors are indispensable to estimate the amount of particle loss. Another sensible aspect of adopting Eq. (8) lies at the steady growing of plane curve. It can be seen that the filtration rate first increases rapidly and then slows down until it reaches a steady stage with an upper limit, rather than continuing increasing to an unknown value.

#### 4.3 Alleviation of filtration effect

In engineering practice, filtration effect contributes greatly to the pressure increment and the reduction of

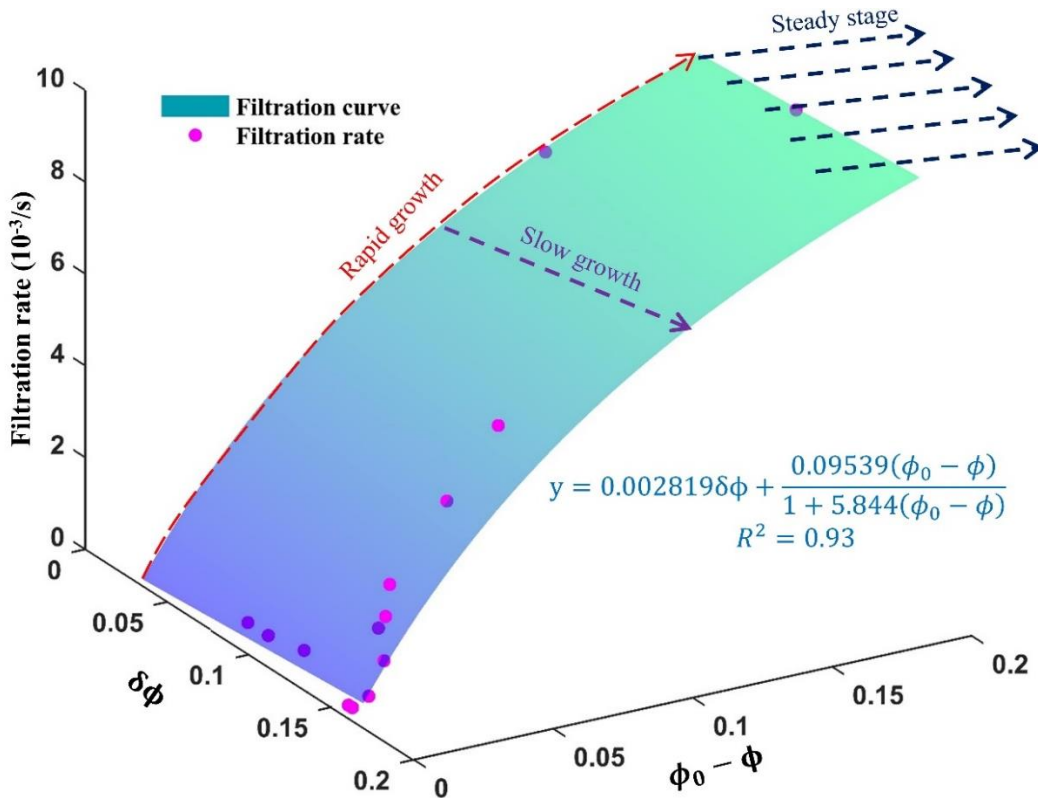


Fig. 9 Evolution of filtration rate considering both volume of cement particles and specific deposition of skeleton

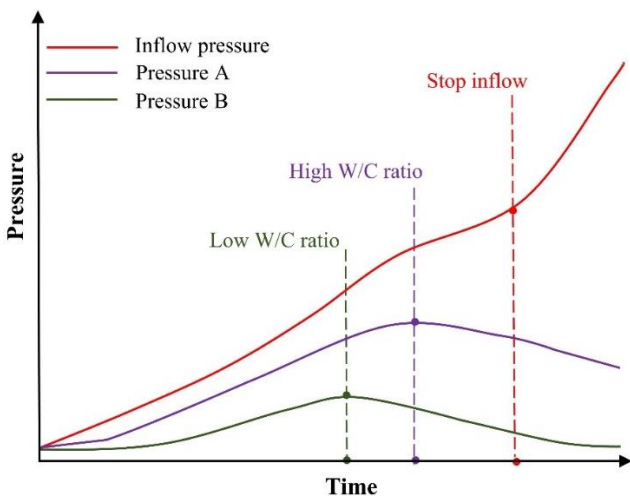


Fig. 10 Schematic illustration of successive grouting scenarios to extend penetration distance

penetration distance in permeation grouting. The success of relieving the filtration effect lies at the extension of penetration distance. Some alternatives such as low-frequency pressure impulse (Ghafar *et al.* 2017) with various types of waves and chemical additions that improves the rheology properties of grout (Sonebi and Perrot 2019), could be adopted to mitigate the filtration behaviour as well. While the essential trigger for the filtration is the large volume of cement particles in flowing grouting, which means that proper grouting sequences and deliberate selection on W/C ratio of grout are likely to enhance the grout ability. A controversial issue is how to

realize an ideal penetration distance while strengthening the porous media with a suitable W/C ratio. Undoubtedly, a more effective consolidation can be reached under a low W/C ratio, and meanwhile, a shorter penetration distance appears. The pressure near the inlet usually becomes extremely high since more cement particles accumulate in this area, and the inflow process needs to be ceased in case of structure damage or fracture caused by excessive pressure. Actually, as discussed before, most voids after the rapid pressure-rising area are far less filled due to the stoppage of the front of the flowing channel that cuts off the grout supply. With the instruction of pressure evolution in different locations, potential stoppage area can be estimated and thus, corresponding W/C ratio of grout could be selected in different periods to alleviate the filtration effect.

One of the options in terms of the grouting scenario is shown in Fig. 10. Instead of relying on the inflow pressure to judge the ceasing time point of the whole grouting process, pressure of two other points along the penetration distance are introduced for reference. The original W/C ratio designed for grouting can be used until pressure B begins to fall down, because the further injection transports little grout through the blockage area but brings about local stoppage. A high W/C ratio of grout is then injected since the diluted grout is more likely to break through the local stoppage and penetrate to a farther distance. Meanwhile, the adoption of a high W/C ratio is able to mitigate the local pressure surge that enhances the risk of fracturing structure, and inject more cement particles without a further boost in filtration effect (El Mohtar *et al.* 2015). The injection process can be terminated after the inflow pressure appears

a step-up and grows speedily, to avoid the damage or crack produced in the injected matrix.

The above scenario can be extended by multiple references of pressure data if more pressure sensors are available along the penetration passage. The successive pressure drop indicates that the gradual stoppage in near-inlet area blocks flowing channels under the initial W/C ratio of grout that possesses a large volume of cement particles. Generally, the solution for the permeability reduction of porous media is based on the initial parameters presented by loose structure and high volume of voids in matrix. The choice of W/C ratio or ceasing criterion may be applicable to unprocessed geological objects, while it would fail to reach the designed target due to the gradually shrinkage of unoccupied flowing channels. Without the direct observation of interior flowing passage, pressure drop is a potential alternative that estimates the effective penetration distance and designates the time point that changes the components of grout or terminates grouting process. Relatively high W/C ratio of grout is extremely appropriate for low-permeability porous media under the same particle size of cement (Axelsson *et al.* 2009). Initial injection of low W/C grout contributes to the sealing of channels with large pore sizes, and hence capturing cement particles evenly during the following high W/C injection. Thus, an early stoppage caused by intensely accumulation over a small area could be avoided.

## 5. Conclusions

To investigate the pressure evolution caused by the filtration of cement particles in permeation grouting, new filtration coefficients involved with the loss rate of cement particles in grout and the dynamic variation rate of deposited particles derived from particles scouring and rolling, was proposed and combined with a convection-filtration model to simulate the pressure evolution. An experiment was designed to obtain the parameters in model and successive pressure drop after the stoppage area was discovered, and then the obtained parameters were used in numerical calculation numerically verify the proposed model. The spatial variation of viscosity and porosity along the penetration distance were considered to explore the evolution of filtration rates. Finally, related application of pressure drop on the alleviation of filtration effect was discussed so as to extend the penetration distance. This work reveals that the nonlinear filtration coefficients are necessary to be considered regarding the filtration-induced pressure evolution and provides a notable approach to mitigate the filtration behaviour. The major conclusions can be drawn as follows:

- Pressure evolution does not follow the continuous increase during permeation grouting. Pressure drop appears once the local area is blocked and cuts off the grout flowing through the blockage. The drop happens successively from the far-inlet area to the inlet, and farther locations see the fall earlier. This can be proved by the fact that the area closer to grout inlet experiences a larger decline on porosity.
- It is apparent that the filtration rate has a strong

relevance with the volume of cement particles and the deposited particles of skeleton. The filtration rate cannot be related by singly considering either of these two factors, neither the linear assumption is applicable to represent the nonlinear trend. Instead, consideration of both these two factors presents a relative ideal result that accords to the experiment.

- The proposed filtration coefficients reveal that the filtration rate grows rapidly at first and then reaches a plateau at which the filtration rate keeps a relatively steady value. The evolution of filtration rate varying with the volume of cement particles under the constant specific deposition basically matches the linear assumption, while the deposited particles of skeleton dominate the filtration behaviour especially under the large accumulation of filtrated particles.

- Partly consideration of inflow pressure may bring about a high risk of fracturing matrix and lowering the grouting efficiency. More references from different locations along the penetration path can be adopted to judge the pressure drop point and accordingly, corresponding change in W/C ratio of grout in drop points is able to mitigate the early stoppage of channels and achieve an ideal penetration distance.

## Acknowledgements

This work was supported by financial grants from the National Basic Research Program of China (2015CB060200), the National Natural Science Foundation of China (41772313), the Hunan Science and Technology Planning Project (2019RS3001) and the Fundamental Research Funds for the Central Universities of Central South University (2018zzts720). The authors are very grateful for the financial contributions and convey their appreciation to the organizations for supporting this basic research.

## References

- Axelsson, M., Gustafson, G. and Fransson, A. (2009), "Stop mechanism for cementitious grouts at different water-to-cement ratios", *Tunn Undergr Sp Tech*, **24**(4), 390-397. <https://doi.org/10.1016/j.tust.2008.11.001>
- Bohlooli, B., Morgan, E.K., Grov, E., Skjolsvold, O. and Hognestad, H.O. (2018), "Strength and filtration stability of cement grouts at room and true tunnelling temperatures", *Tunn Undergr Sp Tech*, **71**, 193-200. <https://doi.org/10.1016/j.tust.2017.08.017>
- Bouchelaghem, F. (2009), "Multi-scale modelling of the permeability evolution of fine sands during cement suspension grouting with filtration", *Comput Geotech*, **36**(6), 1058-1071. <https://doi.org/10.1016/j.compgeo.2009.03.016>
- Bouchelaghem, F. and Almosni, A. (2003), "Experimental determination of the longitudinal dispersivity during the injection of a micro-cement grout in a one-dimensional soil column", *Transport Porous Med*, **52**(1), 67-94. <https://doi.org/10.1023/A:1022376225651>
- Bouchelaghem, F., Vulliet, L., Leroy, D., Laloui, L. and Descoedres, F. (2001), "Real-scale miscible grout injection

- experiment and performance of advection-dispersion-filtration model”, *Int J Numer Anal Met*, **25**(12), 1149-1173. <https://doi.org/10.1002/nag.171>
- Cai, X., Zhou, Z., Liu, K., Du, X. and Zang, H. (2019), “Water-Weakening Effects on the Mechanical Behavior of Different Rock Types: Phenomena and Mechanisms”, *Appl Sci*, **9**(20), 4450. <https://doi.org/10.3390/app9204450>
- Chupin, O., Saiyouri, N. and Hicher, P.Y. (2008), “The effects of filtration on the injection of cement-based grouts in sand columns”, *Transport Porous Med*, **72**(2), 227-240. <https://doi.org/10.1007/s11242-007-9146-z>
- Dang, W., Wu, W., Konietzky, H. and Qian, J. (2019), “Effect of shear-induced aperture evolution on fluid flow in rock fractures”, *Comput Geotech*, **114**, 103152. <https://doi.org/10.1016/j.compgeo.2019.103152>
- Ebrahimi, F. and Barati, M.R. (2018), “Stability analysis of porous multi-phase nanocrystalline nonlocal beams based on a general higher-order couple-stress beam model”, *STRUCT ENG MECH*, **65**(4), 465-476. <https://doi.org/10.12989/sem.2018.65.4.465>
- El Mohtar, C.S., Yoon, J. and El-Khattab, M. (2015), “Experimental study on penetration of bentonite grout through granular soils”, *Can Geotech J*, **52**(11), 1850-1860. <https://doi.org/10.1139/cgj-2014-0422>
- Bidgoli M R, Kolahchi R, Karimi M S. (2016), “An experimental study and new correlations of viscosity of ethylene glycol-water based nanofluid at various temperatures and different solid concentrations”, *STRUCT ENG MECH*, **58**(1), 93-102. <https://doi.org/10.12989/sem.2016.58.1.093>
- Fan, J.C., Liu, W.Y., Liu, C.H., Huang, C.L., Tan, Y.W. and Guo, J.J. (2018), “Evaluating Permeability and Efficiency of Substrates by Using Permeation Grouting Sand Column Test”, *Ksce J Civ Eng*, **22**(8), 2843-2855. <https://doi.org/10.1007/s12205-017-2535-0>
- Ghafari, A., Sadrizadeh, S., Draganovic, A., Johansson, F., Håkansson, U. and Larsson, S. (2017), “Application of Low-Frequency Rectangular Pressure Impulse in Rock Grouting”, *Grouting*, **2**(288), 104-113. <https://doi.org/10.1061/9780784480793.010>
- Ghafari, A.N., Akbar, S.A., Al-Naddaf, M., Draganovic, A. and Larsson, S. (2018), “Uncertainties in Grout Penetrability Measurements; Evaluation and Comparison of Filter pump, Penetrability Meter and Short Slot”, *Geotech Geol Eng*, **36**(2), 747-762. <https://doi.org/10.1007/s10706-017-0351-4>
- Hou, Y.S., Jiang, J.G. and Wu, J.C. (2018), “Characteristic volume fractions of different grains in porous media for anomalous dispersion”, *Environ Fluid Mech*, **18**(6), 1559-1569. <https://doi.org/10.1007/s10652-018-9624-6>
- Im, S.B. and Hurlbaas, S. (2012), “Determination of the repair grout volume to fill voids in external post-tensioned tendons”, *STRUCT ENG MECH*, **42**(1), 25-38. <https://doi.org/10.12989/sem.2012.42.1.025>
- Kim, J.S., Lee, I.M., Jang, J.H. and Choi, H. (2009), “Groutability of cement-based grout with consideration of viscosity and filtration phenomenon”, *Int J Numer Anal Met*, **33**(16), 1771-1797. <https://doi.org/10.1002/nag.785>
- Kim, Y.S. and Whittle, A.J. (2006), “Filtration in a porous granular medium: 1. Simulation of pore-scale particle deposition and clogging”, *Transport Porous Med*, **65**(1), 53-87. <https://doi.org/10.1007/s11242-005-6087-2>
- Kim, Y.S. and Whittle, A.J. (2009), “Particle Network Model for Simulating the Filtration of a Microfine Cement Grout in Sand”, *J Geotech Geoenviron*, **135**(2), 224-236. [https://doi.org/10.1061/\(ASCE\)1090-0241\(2009\)135:2\(224\)](https://doi.org/10.1061/(ASCE)1090-0241(2009)135:2(224))
- Kou, M., Han, D., Xiao, C. and Wang, Y. (2019), “Dynamic fracture instability in brittle materials: Insights from DEM simulations”, *STRUCT ENG MECH*, **71**(1), 65-75. <https://doi.org/10.12989/sem.2019.71.1.065>
- Kou, M., Lian, Y. and Wang, Y. (2019), “Numerical investigations on crack propagation and crack branching in brittle solids under dynamic loading using bond-particle model”, *Eng Fract Mech*, **212**, 41-56. <https://doi.org/10.1016/j.engfracmech.2019.03.012>
- Kou, M., Liu, X., Tang, S. and Wang, Y. (2019), “3-D X-ray computed tomography on failure characteristics of rock-like materials under coupled hydro-mechanical loading”, *THEOR APPL FRACT MEC*, **104**, 102396. <https://doi.org/10.1016/j.tafmec.2019.102396>
- Li, S.-C., Dong, J.-X. and Li, L.-F. (2012), “Experimental hysteretic behavior of in-plane loaded reinforced grouted multi-ribbed aerated concrete blocks masonry walls”, *STRUCT ENG MECH*, **41**(1), 95-112. <https://doi.org/10.12989/sem.2012.41.1.095>
- Liu, R., Liu, Y., Xin, D., Li, S., Zheng, Z., Ma, C. and Zhang, C. (2018), “Prediction of Water Inflow in Subsea Tunnels under Blasting Vibration”, *Water*, **10**(10), 1336. <https://doi.org/10.3390/w10101336>
- Liu, W.J., Zhu, X.H., Zhou, Y.L., Li, T. and Zhang, X.H. (2019), “Bonded-cluster simulation of tool-rock interaction using advanced discrete element method”, *STRUCT ENG MECH*, **72**(4), 469-477. <https://doi.org/10.12989/sem.2019.72.4.469>
- Ma, D., Cai, X., Zhou, Z. and Li, X. (2018), “Experimental investigation on hydraulic properties of granular sandstone and mudstone mixtures”, *Geofluids*, 2018. <https://doi.org/10.1155/2018/9216578>
- Ma, D., Duan, H.Y., Li, X.B., Li, Z.H., Zhou, Z.L. and Li, T.B. (2019), “Effects of seepage-induced erosion on nonlinear hydraulic properties of broken red sandstones”, *Tunn Undergr Sp Tech*, **91**. <https://doi.org/10.1016/j.tust.2019.102993>
- Ma, D., Miao, X.X., Bai, H.B., Pu, H., Chen, Z.Q., Liu, J.F., Huang, Y.H., Zhang, G.M. and Zhang, Q. (2016), “Impact of particle transfer on flow properties of crushed mudstones”, *Environ Earth Sci*, **75**(7). <https://doi.org/10.1007/s12665-016-5382-2>
- Maghous, S., Saada, Z., Dormieux, L., Canou, J. and Dupla, J.C. (2007), “A model for in situ grouting with account for particle filtration”, *Comput Geotech*, **34**(3), 164-174. <https://doi.org/10.1016/j.compgeo.2006.11.003>
- Markou, I.N., Christodoulou, D.N. and Papadopoulos, B.K. (2015), “Penetrability of microfine cement grouts: experimental investigation and fuzzy regression modeling”, *Can Geotech J*, **52**(7), 868-882. <https://doi.org/10.1139/cgj-2013-0297>
- Markou, I.N., Christodoulou, D.N., Petala, E.S. and Atmatzidis, D.K. (2018), “Injectability of Microfine Cement Grouts into Limestone Sands with Different Gradations: Experimental Investigation and Prediction”, *Geotech Geol Eng*, **36**(2), 959-981. <https://doi.org/10.1007/s10706-017-0368-8>
- Moghadas, J., Müller-Steinhagen, H., Jamialahmadi, M. and Sharif, A. (2004), “Theoretical and experimental study of particle movement and deposition in porous media during water injection”, *J Petrol Sci Eng*, **43**(3-4), 163-181. <https://doi.org/10.1016/j.petrol.2004.01.005>
- Nouri, A.Z. and Heydari, M.M. (2017), “Experimental investigation of the effect of baffles on the efficiency improvement of irrigation sedimentation tank structures”, *STRUCT ENG MECH*, **63**(4), 567-574. <https://doi.org/10.12989/sem.2017.63.4.567>
- Park, D. and Oh, J. (2018), “Permeation grouting for remediation of dam cores”, *Eng Geol*, **233**, 63-75. <https://doi.org/10.1016/j.enggeo.2017.12.011>
- Reddi, L.N. and Bonala, M.V. (1997), “Analytical solution for fine particle accumulation in soil filters”, *J Geotech Geoenviron*, **123**(12), 1143-1152. [https://doi.org/10.1061/\(ASCE\)1090-0241\(1997\)123:12\(1143\)](https://doi.org/10.1061/(ASCE)1090-0241(1997)123:12(1143))
- Reddi, L.N., Xiao, M., Hajra, M.G. and Lee, I.M. (2005), “Physical clogging of soil filters under constant flow rate versus

- constant head”, *Can Geotech J*, **42**(3), 804-811. <https://doi.org/10.1139/T05-018>
- Saada, Z., Canou, J., Dormieux, L., Dupla, J.C. and Maghous, S. (2005), “Modelling of cement suspension flow in granular porous media”, *Int J Numer Anal Met*, **29**(7), 691-711. <https://doi.org/10.1002/nag.433>
- Sanderson, R.A., Cann, G.M. and Provis, J.L. (2018), “The effect of blast-furnace slag particle size on the hydration of slag-Portland cement grouts at elevated temperatures”, *Adv Cem Res*, **30**(8), 337-344. <https://doi.org/10.1680/jadcr.17.00136>
- Shabani, A., Jahangiri, H.R. and Shahrabadi, A. (2019), “Data-driven approach for evaluation of formation damage during the injection process”, *J Petrol Explor Prod Technol*, **10**, 699-710. <https://doi.org/10.1007/s13202-019-00764-9>
- Sonebi, M. and Perrot, A. (2019), “Effect of mix proportions on rheology and permeability of cement grouts containing viscosity modifying admixture”, *Constr Build Mater*, **212**, 687-697. <https://doi.org/10.1016/j.conbuildmat.2019.04.022>
- Song, F., Wang, H. and Jiang, M. (2018), “Analytical solutions for lined circular tunnels in viscoelastic rock considering various interface conditions”, *Appl Math Model*, **55**, 109-130. <https://doi.org/10.1016/j.apm.2017.10.031>
- Song, F., Wang, H. and Jiang, M. (2018), “Analytically-based simplified formulas for circular tunnels with two liners in viscoelastic rock under anisotropic initial stresses”, *Constr Build Mater*, **175**, 746-767. <https://doi.org/10.1016/j.conbuildmat.2018.04.079>
- Song, Z., Frühwirt, T. and Konietzky, H. (2020), “Inhomogeneous mechanical behaviour of concrete subjected to monotonic and cyclic loading”, *Int J Fatigue*, **132**, 105383. <https://doi.org/10.1016/j.ijfatigue.2019.105383>
- Song, Z., Konietzky, H. and Herbst, M. (2019), “Bonded-particle model-based simulation of artificial rock subjected to cyclic loading”, *Acta Geotech*, **14**(4), 955-971. <https://doi.org/10.1007/s11440-018-0723-9>
- Sui, W.H., Liu, J.Y., Hu, W., Qi, J.F. and Zhan, K.Y. (2015), “Experimental investigation on sealing efficiency of chemical grouting in rock fracture with flowing water”, *Tunn Undergr Sp Tech*, **50**, 239-249. <https://doi.org/10.1016/j.tust.2015.07.012>
- Tien, C. and Payatakes, A.C. (1979), “Advances in Deep Bed Filtration”, *Aiche J*, **25**(5), 737-759. <https://doi.org/10.1002/aic.690250502>
- Vaz, A., Bedrikovetsky, P., Fernandes, P.D., Badalyan, A. and Carageorgos, T. (2017), “Determining model parameters for non-linear deep-bed filtration using laboratory pressure measurements”, *J Petrol Sci Eng*, **151**, 421-433. <https://doi.org/10.1016/j.petrol.2017.01.001>
- Wang, Q.B., Zhu, Q.K., Shao, T.S., Yu, X.G., Xu, S.Y., Zhang, J.J. and Kong, Q.L. (2018), “The rheological test and application research of glass fiber cement slurry based on plugging mechanism of dynamic water grouting”, *Constr Build Mater*, **189**, 119-130. <https://doi.org/10.1016/j.conbuildmat.2018.08.081>
- Wang, S., Huang, L. and Li, X. (2020), “Analysis of rockburst triggered by hard rock fragmentation using a conical pick under high uniaxial stress”, *Tunn Undergr Sp Tech*, **96**, 103195. <https://doi.org/10.1016/j.tust.2019.103195>
- Wang, S., Li, X., Yao, J., Gong, F., Li, X., Du, K., Tao, M., Huang, L. and Du, S. (2019), “Experimental investigation of rock breakage by a conical pick and its application to non-explosive mechanized mining in deep hard rock”, *Int J Rock Mech Min*, **122**, 104063. <https://doi.org/10.1016/j.ijrmm.2019.104063>
- Wang, Y.-T., Zhou, X.-P. and Kou, M.-M. (2019), “Three-dimensional numerical study on the failure characteristics of intermittent fissures under compressive-shear loads”, *Acta Geotech*, **14**(4), 1161-1193. <https://doi.org/10.1007/s11440-018-0709-7>
- Wang, Y., Zhou, X. and Kou, M. (2019), “An improved coupled thermo-mechanic bond-based peridynamic model for cracking behaviors in brittle solids subjected to thermal shocks”, *EUR J MECH A-SOLID*, **73**, 282-305. <https://doi.org/10.1016/j.euromechsol.2018.09.007>
- Wang, Y., Zhou, X., Wang, Y. and Shou, Y. (2018), “A 3-D conjugated bond-pair-based peridynamic formulation for initiation and propagation of cracks in brittle solids”, *INT J SOLIDS STRUCT*, **134**, 89-115. <https://doi.org/10.1016/j.ijsolstr.2017.10.022>
- Xu, T. and Bezuijen, A. (2019), “Pressure infiltration characteristics of bentonite slurry”, *Geotechnique*, **69**(4), 364-368. <https://doi.org/10.1680/jgeot.17.T.026>
- Yan, Y., Lin, Y., Cheng, J. and Ni, Z. (2017), “Motion behavior research of liquid micro-particles filtration at various locations in a rotational flow field”, *STRUCT ENG MECH*, **62**(2), 163-170. <https://doi.org/10.12989/sem.2017.62.2.163>
- Yang, H. and Balhoff, M.T. (2017), “Pore-network modeling of particle retention in porous media”, *Aiche J*, **63**(7), 3118-3131. <https://doi.org/10.1002/aic.15593>
- Yoon, J. and El Mohtar, C.S. (2014), “Groutability of Granular Soils Using Bentonite Grout Based on Filtration Model”, *Transport Porous Med*, **102**(3), 365-385. <https://doi.org/10.1007/s11242-014-0279-6>
- Yoon, J. and El Mohtar, C.S. (2015), “A filtration model for evaluating maximum penetration distance of bentonite grout through granular soils”, *Comput Geotech*, **65**, 291-301. <https://doi.org/10.1016/j.compgeo.2015.01.004>
- Zhang, C., Zhu, Z., Zhu, S., He, Z., Zhu, D., Liu, J. and Meng, S. (2019), “Nonlinear Creep Damage Constitutive Model of Concrete Based on Fractional Calculus Theory”, *Materials*, **12**(9), 1505. <https://doi.org/10.3390/ma12091505>
- Zhang, M., Dou, L., Konietzky, H., Song, Z. and Huang, S. (2019), “Cyclic fatigue characteristics of strong burst-prone coal: experimental insights from energy dissipation, hysteresis and micro-seismicity”, *Int J Fatigue*, **133**, 105429. <https://doi.org/10.1016/j.ijfatigue.2019.105429>
- Zhou, S.H., Zhang, X.H., Wu, D. and Di, H.G. (2018), “Mathematical Modeling of Slurry Infiltration and Particle Dispersion in Saturated Sand”, *Transport Porous Med*, **124**(1), 91-116. <https://doi.org/10.1007/s11242-018-1054-x>
- Zhou, Z., Wang, H., Cai, X., Chen, L. and Cheng, R. (2019), “Damage Evolution and Failure Behavior of Post-Mainshock Damaged Rocks under Aftershock Effects”, *Energies*, **12**(23), 4429. <https://doi.org/10.3390/en12234429>
- Zhou, Z., Zang, H., Wang, S., Du, X., Ma, D. and Zhang, J. (2018), “Filtration Behaviour of Cement-Based Grout in Porous Media”, *Transport Porous Med*, **125**(3), 435-463. <https://doi.org/10.1007/s11242-018-1127-x>
- Zhou, Z.L., Cai, X., Du, X.M., Wang, S.Y., Ma, D. and Zang, H.Z. (2019), “Strength and filtration stability of cement grouts in porous media”, *Tunn Undergr Sp Tech*, **89**, 1-9. <https://doi.org/10.1016/j.tust.2019.03.015>
- Zhou, Z.L., Cai, X., Li, X.B., Cao, W.Z. and Du, X.M. (2019), “Dynamic Response and Energy Evolution of Sandstone Under Coupled Static-Dynamic Compression: Insights from Experimental Study into Deep Rock Engineering Applications”, *Rock Mech Rock Eng*. <https://doi.org/10.1007/s00603-019-01980-9>
- Zhou, Z.L., Cai, X., Ma, D., Chen, L., Wang, S.F. and Tan, L.H. (2018), “Dynamic tensile properties of sandstone subjected to wetting and drying cycles”, *Constr Build Mater*, **182**, 215-232. <https://doi.org/10.1016/j.conbuildmat.2018.06.056>
- Zhou, Z.L., Du, X.M., Wang, S.Y., Cai, X. and Chen, L. (2019), “Micromechanism of the diffusion of cement-based grouts in porous media under two hydraulic operating conditions: constant flow rate and constant pressure”, *Acta Geotech*, **14**(3), 825-841. <https://doi.org/10.1007/s11440-018-0704-z>

- Zhu, Z., Zhang, C., Meng, S., Shi, Z., Tao, S. and Zhu, D. (2019), "A Statistical Damage Constitutive Model Based on the Weibull Distribution for Alkali-Resistant Glass Fiber Reinforced Concrete", *Materials*, **12**(12), 1908. <https://doi.org/10.3390/ma12121908>
- Zou, L., Håkansson, U. and Cvetkovic, V. (2020), "Yield-power-law fluid propagation in water-saturated fracture networks with application to rock grouting", *Tunn Undergr Sp Tech*, **95**, 103170. <https://doi.org/10.1016/j.tust.2019.103170>
- Zou, L.C., Hakansson, U. and Cvetkovic, V. (2018), "Two-phase cement grout propagation in homogeneous water-saturated rock fractures", *Int J Rock Mech Min*, **106**, 243-249. <https://doi.org/10.1016/j.ijrmms.2018.04.017>
- Zou, L.C., Hakansson, U. and Cvetkovic, V. (2019), "Cement grout propagation in two-dimensional fracture networks: Impact of structure and hydraulic variability", *Int J Rock Mech Min*, **115**, 1-10. <https://doi.org/10.1016/j.ijrmms.2019.01.004>

CC